Microscopic properties of vortex state in YB_6 probed by muon spin rotation

R. Kadono,[1,2] S. Kuroiwa,[3] J. Akimitsu,[3] A. Koda,[1,2] K. Ohishi,[4] W. Higemoto,[4] and S. Otani[5]

[1]*Institute of Materials Structure Science, High Energy Accelerator Research Organization (KEK), Tsukuba, Ibaraki 305-0801, Japan*

[2]*Department of Materials Structure Science, The Graduate University for Advanced Studies, Tsukuba, Ibaraki 305-0801, Japan*

[3]*Department of Physics, Aoyama-Gakuin University, Sagamihara, Kanagawa, 229-8558 Japan*

[4]*Advanced Science Research Center, Japan Atomic Energy Agency, Tokai, Ibaraki 319-1195, Japan*

[5]*Advanced Materials Laboratory, National Institute for Materials Science, Tsukuba, Ibaraki 305-0044, Japan*

(Dated: February 1, 2008)

Local magnetic field distribution $B(\mathbf{r})$ in the mixed state of a boride superconductor, YB_6, is studied by muon spin rotation (μSR). A comparative analysis using the modified London model and Ginzburg-Landau (GL) model indicates that the GL model exhibits better agreement with μSR data at higher fields, thereby demonstrating the importance of reproducing the field profile near the vortex cores when the intervortex distance becomes closer to the GL coherence length. The temperature and field dependence of magnetic penetration depth (λ) does not show any hint of nonlocal effect nor of low-lying quasiparticle excitation. This suggests that the strong coupling of electrons to the rattling motion of Y ions in the boron cage suggested by bulk measurements gives rise to a conventional superconductivity with isotropic s-wave pairing. Taking account of the present result, a review is provided for probing the anisotropy of superconducting order parameters by the slope of λ against field ($\eta \propto d\lambda/dH$).

I. INTRODUCTION

The revelation of superconductivity in magnesium diboride (MgB_2, $T_c \simeq 39$ K) has stimulated renewed interest to other boride superconductors as an alternative path to novel superconductors with ever higher T_c.[1] Among those, yttrium hexaboride (YB_6) currently holds the position of second highest transition temperature ($T_c \geq 7$ K),[2] thereby drawing considerable attention on the detailed mechanism of superconductivity. In particular, it stands as a focus of investigation on the effect of rattling motion of alkaline earth metals contained in a relatively large boron cage that gives rise to anharmonic phonons having relatively low energy ($\simeq 10^1$ meV).[3] A similar situation is reported in a variety of novel superconductors including metal-doped silicon clathrates[4] and β-pyrochlores.[5]

While YB_6 is known as a type II superconductor in which the Ginzburg-Landau (GL) parameter κ ($\equiv \lambda/\xi$, with λ being the magnetic penetration depth and $\xi = \xi_{\rm GL}$ the GL coherence length) is greater than unity, it is characterized by a low upper critical field [$B_{c2} = \mu_0 H_{c2}(0) \simeq 0.3$ T] and associated long ξ ($\sim \xi_0 \simeq 30$ nm, the BCS coherence length) that is only a few times smaller than λ ($\simeq 130$ nm). This means that the volume fraction occupied by vortex cores ($\simeq \pi\xi^2 H/\Phi_0$, where H is the external magnetic field and Φ_0 is the flux quantum) is relatively large in the flux line lattice (FLL) state over the entire field range, making YB_6 an ideal stage for studying the electronic structure of vortex cores in detail. In this situation, it is pointed out that the modified London (m-London) model, which is known to be an excellent analytical model to describe the spatial distribution of magnetic field $B(\mathbf{r})$ for arbitrary κ but *at low magnetic induction* ($B/B_{c2} < 0.25$),[6,7] may not be appropriate for the basis to extract physical parameters out of $B(\mathbf{r})$.[8] One of the primary purposes of the present study is to address this potential problem by making a comparative analysis of μSR data by both m-London and GL models, which reveals that the latter provides systematically better description of magnetic field profile at higher magnetic induction. Thus, it is inferred from this study that we have to resort to the GL model for proper understanding of the FLL state over the wider field range. Fortunately, however, in contrast to the case of classical type II superconductors such as Nb or V ($\kappa \simeq 1$) where one might need numerical approach to obtain $B(\mathbf{r})$ with sufficient precision,[9,10] the present result suggests that an analytical solution of the GL model obtained by variational method[11,12] is sufficient for the system with reasonably large κ.

It must be stressed that the magnetic penetration depth controlling the actual shape of $B(\mathbf{r})$ corresponds to an effective value of the London penetration depth determined by the superfluid density n_s,

$$\frac{1}{\lambda^2} = \frac{4\pi e^2}{m^* c^2} n_s \qquad (1)$$

(where m^* is the effective mass of the charge carriers), so that it may vary according to the change in n_s due to quasiparticle excitations (breaking of the Cooper pairs) of various origins. In particular, it is anticipated that the pair breaking due to the quasiclassical Doppler shift of the Fermi momenta around vortices would lead to the low energy quasiparticle excitation (the nonlinear effect).[13] Considering that the number of vortices is proportional to the external field, it is predicted that n_s is more reduced at higher H due to the Doppler shift. Another important consequence of the anisotropic order parameter is the nonlocal effect due to the variable coherence length [$\xi_0 \equiv \xi_0(\mathbf{k})$] that may exceed the London penetration depth ($\lambda_{\rm L}$) over a certain region of the Fermi

surface, as it is inversely proportional to the order parameter [$\xi_0(\mathbf{k}) \propto \hbar v_{\rm F}/\pi\Delta(\mathbf{k})$, with $v_{\rm F}$ being the Fermi velocity].[14] In this situation, the flow of supercurrent is strongly modified over the region $\lambda_{\rm L} < \xi_0(\mathbf{k})$, leading to the change (expansion) of effective λ.[15] Note that this is not limited to the case of nodal gap, but would be in effect for anisotropic gap (or multi-gapped) with the minimum gap satisfying $\Delta_{\rm min} < \hbar v_{\rm F}/\pi\lambda_{\rm L}$. Meanwhile, multi-gapped superconductors have a multitude of coherence length and associated vortex core radius within which the quasiparticles are confined. The presence of quasiparticles over the region of larger vortex cores would serve as a factor to enhance the effective λ more strongly at lower fields, thus mimicking the above mentioned Volovik effect without gap nodes.

We have shown that the magnetic field dependence of λ provides a useful criterion to assess the anisotropy of superconducting order parameter; the greater field gradient ($d\lambda/dH$) corresponds to stronger anisotropy or multi-gapped structure in the order parameter.[16] We demonstrate in YB_6 that λ deduced from the GL model-based analysis does not depend on the external magnetic field. This provides strong microscopic evidence for the isotropic superconducting gap in YB_6.

II. MODELS FOR THE FIELD PROFILE

In the conventional μSR studies of the FLL state, positive muons are implanted to the superconducting specimen with their initial spin polarization perpendicular to the external magnetic field [$\hat{P}(0) \perp \vec{H}$, with $\vec{H} \parallel \hat{z}$ in the following], so that they may probe $B(\mathbf{r})$ [$\equiv B_z(\mathbf{r})$] generated by a periodic array of magnetic vortices which are apart by $a_0 \simeq \sqrt{\Phi_0/H\sin\theta}$ (with the apex angle $\theta = 60^\circ$ for the hexagonal FLL and $= 90^\circ$ for the square FLL). Considering that muon stops at the interstitial sites in the atomic unit cell of the crystalline lattice which has a periodicity much shorter than that of vortices ($a_0 \geq 89$ nm for $\mu_0 H \leq 0.3$ T assuming a hexagonal FLL), one can presume that μSR signal in the FLL state provides a random sampling of $B(\mathbf{r})$,

$$\begin{aligned} \hat{P}(t) &= P_x(t) + iP_y(t) \\ &= \int_{-\infty}^{\infty} n(B)\exp(i\gamma_\mu Bt - i\phi)dB, \qquad (2) \\ n(B) &= \langle\delta(B - B(\mathbf{r}))\rangle_{\mathbf{r}}, \qquad (3) \end{aligned}$$

where $n(B)$ is the spectral density for the internal field defined as a spatial average ($\langle\rangle_{\mathbf{r}}$) of the delta function, γ_μ is the muon gyromagnetic ratio ($= 2\pi \times 135.53$ MHz/T), and ϕ is the initial phase of rotation.[6] These equations indicate that the real amplitude of the Fourier transformed muon spin precession signal, $\mathrm{Re}\int \hat{P}(t)\exp(-i\gamma_\mu Bt)\gamma_\mu dt$, corresponds to the spectral density, $n(B)$.

In general, $B(\mathbf{r})$ is obtained by solving the GL equation for the field profile and the order parameter $\psi(\mathbf{r})$ in the self-consistent manner, which usually requires numerical approach. However, in the case of strong type II superconductors ($\kappa \gg 1$), the nonlocal character is confined within the immediate vicinity of vortex cores ($|\mathbf{r}| \leq \xi_{\rm GL}$) and the London approximation can be extended by introducing a cutoff factor associated with the vanishing $\psi(\mathbf{r})$ at the vortex center. In the modified London model, $B(\mathbf{r})$ satisfies the equation

$$B(\mathbf{r}) - \mathrm{curl}[\hat{\Lambda}\cdot\mathrm{curl}B(\mathbf{r})] = \Phi_0\sum_i \rho(\mathbf{r} - \mathbf{r}_i), \qquad (4)$$

where $\hat{\Lambda}$ is the tensor related to the penetration depth and $\rho(\mathbf{r})$ is the source term for the vortices located at the position $\mathbf{r}_i$ in the lattice. The solution is given by a sum of the magnetic induction from isolated vortices to yield

$$\begin{aligned} B(\mathbf{r}) &= \sum_{\mathbf{K}} b(\mathbf{K})\exp(-i\mathbf{K}\cdot\mathbf{r}) \qquad (5) \\ b(\mathbf{K}) &= \frac{B_0}{1 + \mathbf{K}\hat{L}\mathbf{K}} F(K, \xi_{\rm c}), \qquad (6) \end{aligned}$$

where $\mathbf{K}$ are the vortex reciprocal lattice vectors, B_0 ($\simeq \mu_0 H$) is the average internal field, $\hat{L}(\mathbf{K})$ is the *effective* London penetration depth, $F(K, \xi_{\rm c})$ is the cutoff factor (with $\xi_{\rm c} \propto \xi$ being the cutoff parameter) to remove the unphysical divergence in the magnetic field distribution near the vortex center: The local London approximation, $\rho(\mathbf{r}) = \delta(\mathbf{r})$, corresponds to $F(K, \xi_c) = 1$, where $B(\mathbf{r})$ exhibits a logarithmic divergence. The local approximation also leads to the reduction of the term $\mathbf{K}\hat{L}\mathbf{K}$ into λ^2K^2 corresponding to the isotropic Fermi surface. Here, "local" implies that the electromagnetic interaction does not depend on the wave vector ($\mathbf{K}$), whereas that referring to the source term is primarily meant for $\xi_c = 0$. The form of $F(K, \xi_{\rm c})$ depends on the modelling of $\rho(\mathbf{r})$ and associated $\psi(\mathbf{r})$ in the vicinity of vortex cores. For example, the Gaussian cutoff,

$$F(K, \xi_{\rm c}) = \exp\left(-\frac{1}{2}K^2\xi_c^2\right), \qquad (7)$$

which is widely used for μSR data analysis (valid for $B/B_{c2} < 0.25$ and $\kappa \gg 1$), is derived by the isotropic GL theory from the Gaussian source term in the London equation[6,17]

$$\rho(\mathbf{r}) = \frac{\Phi_0}{2\pi\xi_0^2}\exp\left(-\frac{r^2}{2\xi_0^2}\right). \qquad (8)$$

Although this form is presumed to be valid only in the GL limit (i.e., near T_c), it is known that Eq. (7) reproduces the cutoff function derived from the most commonly assumed form of the order parameter that fits well the solution of the Bogoliubov-de Gennes (BdG) equation,

$$\psi(r) = \psi_\infty \tanh\frac{r}{\xi}. \qquad (9)$$

We also note that a renormalzation factor, $\sqrt{1-b}$ (where $b \equiv B/B_{c2}$), was introduced to the m-London model in

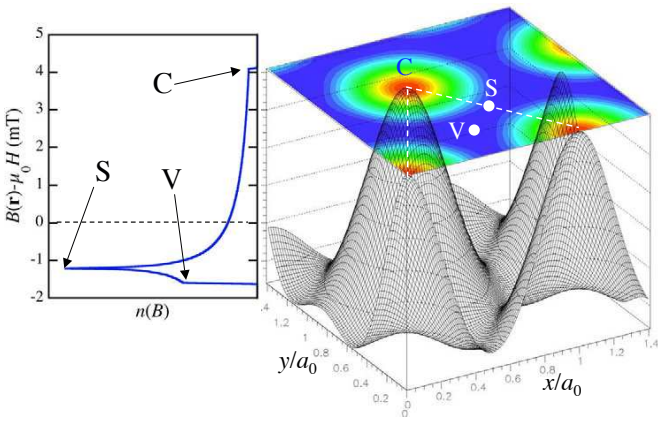

FIG. 1: Density distribution function ($n(B)$, left) and corresponding spatial field profile ($B(\mathbf{r})$, right) for a hexagonal flux line lattice obtained from the Ginzburg-Landau model; $\lambda = 125$ nm, $\xi = 30$ nm, and $B_0 = 0.15$ T. The distance between flux lines, a_0, is 12.6 nm. The points marked as 'C', 'S', 'V' in $n(B)$ respectively correspond to those in $B(\mathbf{r})$. Thus, despite its one-dimensionality, $n(B)$ has a site-selective sensitivity in the unit cell of FLL.

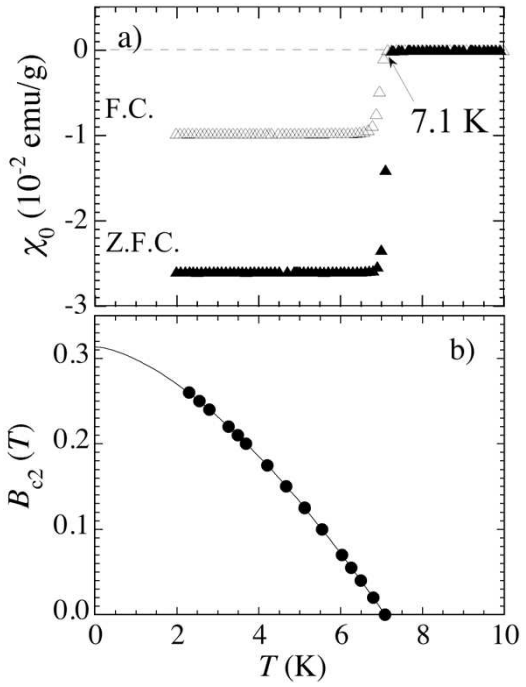

FIG. 2: Superconducting transition in YB_6 observed by (a) magnetic susceptibility ($\mu_0 H = 1$ mT), and (b) the upper critical field determined by specific heat. Solid curve in (b) is fit by a power law (see text).

the earlier literatures to account for the reduction of the GL order parameter at higher fields (see below), where λ and ξ_c in Eq. (6) are divided by this factor.[6,8] However, it turns out throughout this work that this renoramlization is too strong to be consistent with our experimental observation, and therefore disregarded in the following analysis.

On the other hand, an approach using variational method has been made to obtain the analytical GL solution for $B(\mathbf{r})$ by assuming

$$\psi(r) = \psi_\infty \frac{r}{\sqrt{r^2 + \xi_v^2}}, \tag{10}$$

which leads to a squared Lorentzian source term[15]

$$\rho(\mathbf{r}) = \frac{\Phi_0}{\pi} \frac{\xi_v^2}{(r^2 + \xi_v^2)^2}, \tag{11}$$

and associated cutoff function (for $B \ll B_{c2}$)

$$F(K, \xi_v) = uK_1(u), \;\; u = \sqrt{K^2\xi_v^2 + \xi_v^2/\lambda^2}, \tag{12}$$

where $K_1(x)$ is the modified Bessel function and $\xi_v \simeq \sqrt{2}\xi_0$ is the variational parameter.[11] This model was extended to higher fields and to anisotropic order parameters by Hao *et al.*[18] to consider the reduction of order parameter due to the overlap of vortex cores, yielding the Fourier component

$$b(\mathbf{K}) = B_0 \frac{vK_1(u)}{uK_1(v)}, \;\; u = \sqrt{K^2\xi_v^2 + v^2}, \; v = \frac{\xi_v}{\lambda} f_\infty, \tag{13}$$

where ξ_v and f_∞ are the variational parameters with the latter representing the field-dependent order parameter ($\psi_\infty \to f_\infty \psi_\infty$; $f_\infty \to 1$ for the dilute vortex limit). Under a condition of $\lambda^2 K_{\rm min}^2 \gg 1$, where $\mathbf{K}_{\rm min}$ is the smallest nonzero reciplocal lattice vector, Eq. (13) is simplified for the extreme type II case ($\kappa \gg 1$) using an approximation $K_1(x) \simeq 1/x$ to yield[12]

$$b(\mathbf{K}) \simeq B_0 f_\infty^2 \frac{uK_1(u)}{\lambda^2 K^2}, \tag{14}$$

where

$$f_\infty^2 \;=\; 1 - b^4, \;\; b \equiv B/B_{c2} \tag{15}$$

$$u^2 \;=\; K^2\xi_v^2 \simeq 2K^2\xi^2(1+b^4)[1-2b(1-b)^2]. \tag{16}$$

In the present case of YB_6, $K_{\rm min}$ for a hexagonal FLL is $4\sqrt{3}/a_0 \simeq 0.015$ nm^{-1} (where $a_0 \simeq 455$ nm for the lowest field $B_{c1} \simeq 0.02$ T), which leads to $\lambda^2 K_{\rm min}^2 \simeq 3.9$ ($\lambda \simeq 130$ nm), indicating that $\lambda^2 K_{\rm min}^2$ is considerably greater than unity. Moreover, $K_{\rm min}^2 \xi^2 \simeq 0.2$ ($\xi \simeq 30$ nm), which is again larger than $v^2 \le \kappa^{-2} \simeq 0.05$ to justify the approximation, $u \simeq K\xi_v$ [see Eq. (13)]. Thus, YB_6 satisfies the conditions for Eqs. (14)–(16) to be employed as a model to describe $B(\mathbf{r})$.

An example of $B(\mathbf{r})$ and corresponding $n(B)$ calculated by the GL model is shown in Fig. 1. Regardless of the details in the modeling of $B(\mathbf{r})$, it predicts an asymmetric field profile for $n(B)$ characterized by a negatively shifted sharp peak due to the van Hove singularity associated with the saddle points of $B(\mathbf{r})$ (marked as 'S' in Fig. 1), and an adiabatic tail towards higher fields where

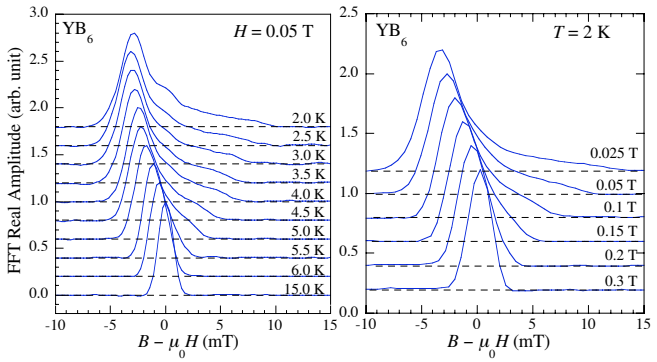

FIG. 3: Real amplitude of the fast Fourier transform (FFT) of μSR time spectra under several temperature/magnetic fields ($\mu_0 H$) in the mixed state of YB_6 (corresponds to $n(B)$). The small bump at $B-\mu_0 H = 0$ seen in the spectra at low temperature/field is due to background signal from muons stopped in the sample holder.

the maximal field is determined by $B(|\mathbf{r} - \mathbf{r}_i| \sim \xi)$. The nearly one-to-one correspondence between the characteristic points of $n(B)$ and those on $B(\mathbf{r})$ makes it feasible to deduce complex physical parameters including λ and ξ from a single μSR spectrum. Meanwhile, information on the structure of FLL must be provided by other techniques (e.g., small angle neutron scattering). Since no such information seems to be available for YB_6, we presume in the following that a hexagonal FLL is realized.

While one might argue that the m-London model should be replaced by the GL model simply because of the wider field range of applicability, we point out that the physical meaning of ξ_v in the GL model has some uncertainty in the sense that it has a complicated field dependence as a cutoff parameter [see Eq. (16)], yielding different values at different fields for a common ξ. This casts some ambiguity, particularly on the behavior of vortex core radius as a function of external field. The GL model has another disadvantage in the practical application that it requires significant computing resources (CPU power, in particular) for the precise treatment. The m-London model, in contrast, is relatively free from such ambiguity of model parameters, and it can be implemented with ordinary computing environment. Thus, the m-London model would remain to be a useful basis for the application of μSR to the study of the mixed state, as far as precaution is taken on the limit of its validity.

Finally, it may be worthy of mention that $F(K, \xi_v)$ would be also dependent on the details of the Fermi surface, and thereby it may be subject to further correction to include $\mathbf{K}$ dependence.[19] While the effect of such anisotropy within the vortex cores may be small at the dilute vortex limit, it may be important at fields close to B_{c2} in anisotropic superconductors.

III. EXPERIMENTAL DETAILS

Single crystals of YB_6 were prepared by the floating zone technique, where the details of the crystal growth is found elsewhere.[20] Magnetization, specific heat, and electronic resistivity were measured prior to μSR experiment to evaluate the bulk properties of the specimen. As shown in Fig. 2, the result indicates that the crystal has a superconducting transition temperature of $T_c = 6.95(15)$ K (defined at the midpoint of change in χ_0) and an upper critical field of $B_{c2}(0) = 0.31$ T. Other physical properties deduced from those measurements are summarized in Table I. The ratio $2\Delta(0)/k_B T_c \simeq 3.67$ (deduced from the jump of the electronic specific heat at T_c) is close to the BCS value of 3.53. The mean-free path is estimated to be ∼2.83 nm from the residual resistivity ratio. This is much shorter than ξ_0 $[= (\Phi_0/2\pi B_{c2}(0))^{1/2}]$, thereby indicating that the superconductivity is in the dirty limit. This strongly suggests that nonlocal effect in terms of $\mathbf{K}$ dependence, if it exists at all, must be masked by the impurity scattering in this specimen.

Conventional μSR measurements under a transverse field (TF) were carried out on the M15 beamline at the Tri-University Meson Facility (TRIUMF, Vancouver, Canada), where the field direction was perpendicular to the crystal plane (normal to [001] axis) covering an area of 8 mm × 8 mm on the sample holder ($H \parallel \hat{z}$ and [001]). A positive muon beam with the initial polarization normal to the $\hat{z}$ axis was implanted into the specimen, and the time evolution of muon spin polarization $[\hat{P}(t)]$ was monitored by detecting the decay positrons emitted preferentially towards the direction of $\hat{P}(t)$. Each measurement was done by accumulating $2 \sim 4 \times 10^7$ positron events on two pairs of scintillation counters (for $\hat{x}$ and $\hat{y}$ directions) that yield μSR signals

$$\hat{A}(t) = A_x(t) + iA_y(t) = A_0 \hat{P}(t), \qquad (17)$$

where $A_x(t)$ and $A_y(t)$ are the decay positron asymmetry for the respective pair of counters with A_0 being the total asymmetry. Measurements on the vortex state were made under field-cooled conditions to minimize the effect of flux pinning that may give rise to additional broadening of the μSR lineshape.

T_c (K)	$\frac{2\Delta(0)}{k_B T_c}$	rrr	B_{c1} (mT)	B_{c2} (T)	l (nm)	λ_L (nm)	ξ_0 (nm)
6.95(15)	3.67	4.62	18.5	0.31	2.83	134(2)	33(1)

TABLE I: Bulk properties of YB_6 used for the μSR experiment, where T_c is the superconducting transition temperature (defined by the midpoint of χ_0), $\Delta(0)$ is the energy gap extrapolated to zero temperature, rrr is the residual resistivity ratio, B_{c1} and B_{c2} are the lower and upper critical field, l is the mean free path (deduced from rrr), λ_L is the London penetration depth (from B_{c1}), and ξ_0 is the BCS coherence length (from B_{c2}).

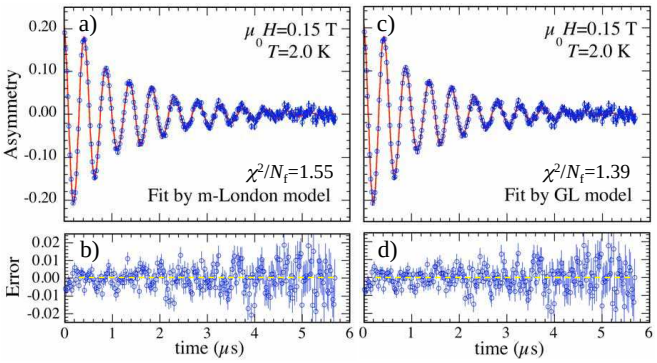

FIG. 4: Time revolution of μ-e decay asymmetry [$A_x(t)$, circles] in YB_6 at $\mu_0 H = 0.15$ T and T=2.0 K displayed on a rotating reference frame of 18 MHz, where solid curves in a) and c) are fits assuming $B(\mathbf{r})$ obtained by the m-London model ($\lambda = 153$ nm, $\xi_c = 25.6$ nm) and GL model ($\lambda = 123$ nm, $\xi = 29.6$ nm), respectively. Fit errors are shown in b) and d) as difference patterns between data and fit.

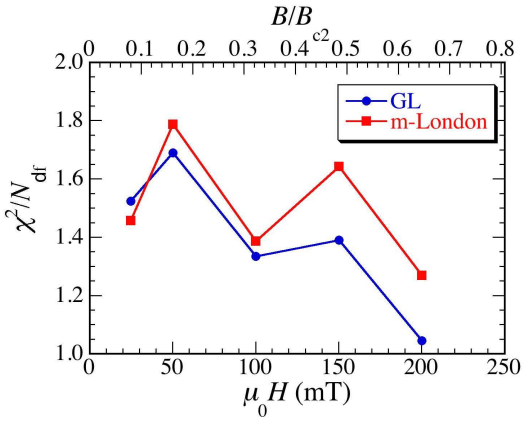

FIG. 5: Residual χ^2 divided by the number of degree of freedom ($N_{\rm df}$).

IV. RESULT

A. Comparison of models: Field dependence of λ and ξ

Examples of the fast Fourier transform (FFT) of μSR spectra at several external magnetic fields are shown in Fig. 3, where one can readily observe the asymemtric lineshape with slight smearing due to the limited time window for FFT (0–6 μs). The peaks at lower field represent the van Hove singularity due to the saddle points of $B(\mathbf{r})$ ('S' in Fig. 1). additional peak at $B - \mu_0 H = 0$ is due to muons which missed the specimen and stopped in the positron counters surrounding the specimen. The value of $\mu_0 H$ is experimentally determined by the spectrum of each field above T_c. Based on the least-square method with appropriate consideration of the statistical uncertainty, the μSR spectra are compared (in time domain) with those calculated by using Eqs.(2)–(6),

$$\hat{A}(t) = A_0 \int_{-\infty}^{\infty} [(1 - f_{\rm b}) e^{-(\sigma_{\rm p}^2 + \sigma_{\rm n}^2)t^2} n(B) + f_{\rm b}\delta(B - \mu_0 H)] e^{i\gamma_\mu B t - i\phi} dB, \qquad (18)$$

from which a set of parameters for $n(B)$, λ, and ξ_c [or ξ in Eq. (16) for the GL model] is deduced. Here, $\sigma_{\rm p}$ is the additional relaxation due to random flux pinning, $\sigma_{\rm n}$ is that due to random local fields from nuclear magnetic moments, and $f_{\rm b}$ denotes the fractional yield of the background signal. $\sigma_{\rm n}$ ($\simeq 0.17$ MHz) was determined from the μSR spectrum above T_c, and $f_{\rm b}$ was less than 3 % of the total asymmetry. The background comes from muons stopping in the positron counters (which survived due to the finite deficiency of *veto* logic circuits to eliminate such positron events) and thereby showing negligibly small relaxation rate. We found that the average internal field (B_0) showed a small positive shift (≤ 1 mT) from the external field ($\mu_0 H$) with randomly varying magnitude. We attribute this to the effect of random pinning of vortices and associated demagnetization which seems to be strong in this specimen as suggested by relatively large σ_p ($\simeq$0.2–0.5 MHz at any field/temperature). Thus, we allowed B_0 to vary slightly (≤ 1 mT) to obtain the best fit. Fig. 4 shows an example of analysis in the time domain, where fits by the m-London and GL models are displayed for the data at $\mu_0 H = 0.15$ T and $T = 2.0$ K. Although both models yield reasonable fit to data, the ratio of χ^2 to the number of degree of freedom is considerably reduced from 1.55 for the m-London model to 1.39 for the GL model: one may observe the scatter in b) is slightly reduced in d). As is evident in Fig. 5, this tendency is more clearly observed at higher fields, and it is consistent with the presumption that the GL model provides better description over the higher field region. Meanwhile, it should be also stressed that both models yield almost the same quality of fits at lower fields ($b \leq 0.3$).

Figure 6 shows comparison between those two models for the profiles of $B(r)$, supercurrent calculated by the Maxwell's relation,

$$J(r) = \mathrm{curl}\{B(r)\} = \frac{dB_z(r)}{dx} - \frac{dB_z(r)}{dy}, \qquad (19)$$

and superconducting order parameter $[\psi(r)/\psi(\infty)]$ plotted along the straight line connecting the nearest-neighbor vortices, where the curves in (a)–(b) and (d) are calculated by using parameters obtained by fits shown in Fig. 4. The field profile generated by the GL model keeps increasing towards the vortex center beyond that by m-London model, yielding smaller effective radius (r_0) for vortex cores defined by the peak of the supercurrent [$J(r_0) = |J|_{\rm max}$ with $r_0 \simeq 25$ nm for GL and $\simeq 30$ nm for m-London]. Note that the definition of ξ in the GL model is quite different from ξ_c in the m-London model, and thus they cannot be compared directly. Meanwhile, r_0 is defined directly from the field profile using Eq. (19), and thereby it serves as a common ground for comparison of vortex core size. It is noteworthy that, despite

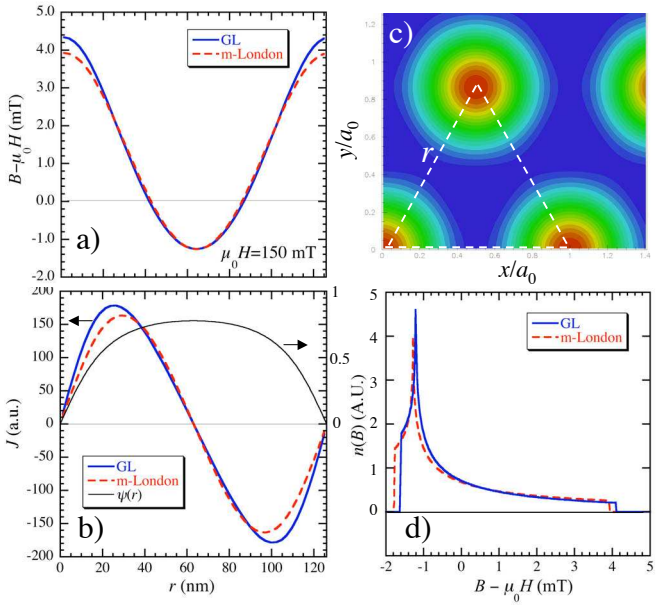

FIG. 6: (a) The spatial field profile of $B(r)$ along the straight line connecting nearest neighboring vortices [shown in (c) by dashed line], where λ and ξ_c (ξ) are taken respectively from the result of fits shown in Fig 4. (b) The spatial profile of the supercurrent obtained by the Maxwell's relation [$J(r) = \mathrm{curl}B(r)$]. The normalized order parameter [$\overline{\psi}(r) = \psi(r)/\psi(\infty)$] calculated by Eq. (10) is also plotted. (d) The density distribution $n(B)$ corresponding to each curve in (a).

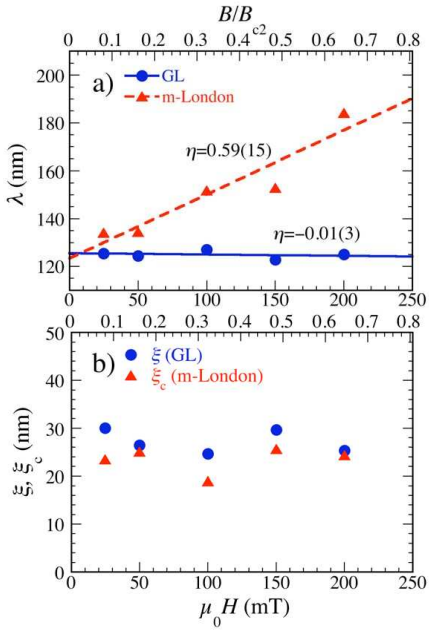

FIG. 7: Magnetic field dependence of penetration depth and cutoff parameter as determined from the m-London and the GL models. The solid and dashed lines are linear fits to the data obtained by the respective models.

relatively small value of b ($\simeq 0.5$), the order parameter in Fig. 6(b) calculated as a product of Eq. (10) for two neighboring vortices exhibits considerable reduction at the center between two vortices. This again suggests that the GL model must be used for the proper description of FLL state over the relevant field range.

While the difference between two models appears to be localized in the field profile near the vortex cores, it gives rise to change in the deduced value of λ. As shown in Fig. 7(a), those obtained by the m-London model exhibits a clear tendency of longer λ at higher fields than m-London model. A similar result is reported for the case of $NbSe_2$ (see Fig. 32 of Ref. [8]), although the data are limited to lower fields ($b < 0.31$). In the case of YB_6, this leads to qualitative difference in the dimensionless paramater, η, to describe the gradient of λ against field, which is defined as

$$\lambda(b) = \lambda(0)[1 + \eta \cdot b]. \qquad (20)$$

Fits of data in Fig. 7(a) using the above relation yields $\eta = 0.59(3)$ for the m-London model and $\eta = -0.01(3)$ for the GL model. Since it is anticipated that $\eta \simeq 0$ for the case of isotropic order parameter, the analysis by the GL model, which provides better description of $B(\mathbf{r})$, implies that YB_6 belongs to the class of conventional BCS superconductors with isotropic energy gap. This in turn indicates that a precaution must be taken upon evaluating the magnitude of η to employ model appropriate for the relevant field range of data. We will come back to this issue later below.

In contrast to the case of λ, there is not much difference in the field dependence of cutoff parameters between two models, where both ξ_c and ξ fall into similar values between 20 and 30 nm. While ξ shows a weak tendency of decrease with increasing field, ξ_c does not show any clear trend. As mentioned earlier, the corresponding vortex core radius defined as the peak position of supercurrent is slightly smaller than ξ in the GL model, while an opposite tendency is observed for the case of m-London model. Taking an average of ξ over the observed field range [= 27(2) nm], we obtain the corresponding GL parameter $\kappa = 4.7(4)$ in good agreement with $\kappa \simeq 4.1$ from the bulk property measurements. The fact that both λ and ξ are independent of H means that κ is also a constant against H.

B. Temperature dependence of λ and ξ

Figure 8 shows the temperature dependence of $1/\lambda^2$ and ξ determined by the fits of μSR spectra at $\mu_0 H = 0.05$ T, using solutions of the GL model for generating $n(B)$. Since we showed in the previous section that the GL model is superior to m-London model, we focus on the result of analysis by the GL model in the following.

The solid curve in Fig. 8(a) is a fit by the weak coupling

BCS theory

$$\frac{1}{\lambda^2(T)} = \frac{1}{\lambda^2(0)}\left[1 - 2\int_{\Delta}^{\infty}\left(-\frac{df}{dE}\right)\frac{EdE}{\sqrt{E^2-\Delta^2}}\right], \quad (21)$$

where $f(E)$ is the Fermi distribution function and $\Delta = \Delta(T)$ is the temperature-dependent gap energy. It reproduces data reasonably well, yielding $\lambda(0) = 123(2)$ nm and $T_c = 6.2(1)$ K. The obtained T_c is in excellent agreement with that determined by bulk measurements at $\mu_0 H = 0.05$ T shown in Fig. 2(b). The scatter of data points might be attributed to the relatively strong pinning that might give rise to a distortion of $B(\mathbf{r})$ that is beyond the limit of Gaussian approximation [i.e., $\exp(-\sigma_{\rm p}^2 t^2)$, see the inset of Fig. 8(a)]. Although the absence of data below 2 K does not allow definite conclusion, the temperature dependence of $1/\lambda^2$ is consistent with the conventional BCS model for isotropic s-wave pairing, supporting the conclusion drawn from the field dependence of λ.

The temperature dependence of ξ is displayed in Fig. 8(b). It exhibits a tendency of decrease with decreasing temperature and saturates below $T \leq 4$ K. Similar results are reported for the cases of $NbSe_2$ (Ref.21) and V (Ref.10), where the observed temperature dependence has been attributed to the so-called Kramer-Pesch effect.[22] In the FLL state, the order parameter serves as a potential energy [$\propto \psi(r)$, the pair potential] for the quasiparticles, and they are trapped in the vortex cores (by the Andreev reflection) to form discrete energy levels. In clean superconductors, it is then predicted that the vortex core radius ($\propto \xi$) must be dependent on temperature, because the higher energy levels, which are occupied by quasiparticles at higher temperatures, have greater extension corresponding to a larger core size. Unfortunately, however, the experimentally observed temperature dependence of ξ seems to be much weaker than the predicted linear dependence, $\xi \sim \xi_0 \cdot (T/T_c)$, in those earlier examples which are in the clean limit. Meanwhile, it is predicted that the effect is sensitive to the impurity scattering and thereby it would be smeared out in the dirty limit corresponding to the present case of YB_6. This is again in contrast to the observed behavior of ξ for $T \geq 4$ K, suggesting that it cannot be attributed to the Kramer-Pesch effect.

Here, we recall a much simpler argument that the weak temperature dependence of ξ can be naturally explained by considering the fact that B_{c2} varies with temperature.[23] Since the GL coherence length near T_c is given by the relation

$$\xi_{\rm GL}(T) = \sqrt{\frac{\Phi_0}{2\pi B_{c2}(T)}}. \quad (22)$$

it is natural to assume $\xi(T) \simeq \xi_{\rm GL}(T) \propto [B_{c2}(T)]^{-1/2}$. Thus, the increase of ξ at higher temperatures might be attributed to the decrease of $B_{c2}(T)$. A fit of $B_{c2}(T)$ in Fig. 2(b) by a power law,

$$B_{c2}(T) = B_{c2}(0)[1 - \zeta(T/T)^{\nu}], \quad (23)$$

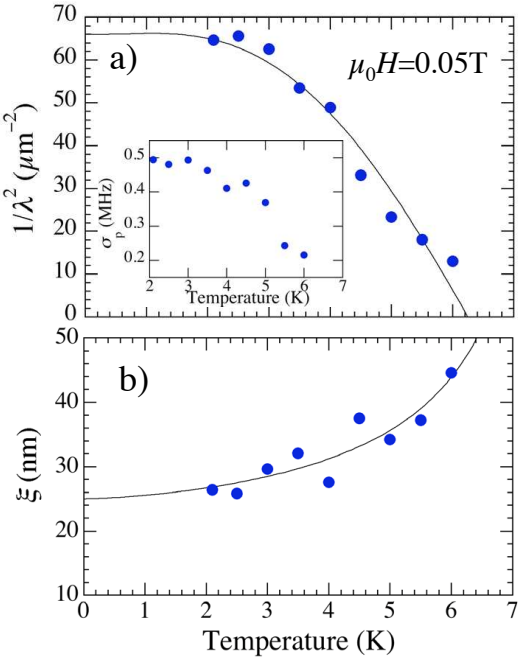

FIG. 8: Temperature dependence of $1/\lambda^2$ (a) and cutoff parameter (b) as determined from the GL model. Solid curve in (a) is a fit by the weak coupling BCS theory, and that in (b) is fit by a power law proportional to $[B_{c2}(T)]^{-1/2}$ (see text). Inset: The rate of additional relaxation due to flux pinning.

yields $B_{c2}(0) = 0.314(1)$ T, $\zeta = 0.970(1)$ and $\nu = 1.56(1)$ The solid curve in Fig. 8(b) is the best fit obtained by assuming Eq. (22) and (23) with the above parameter values, which yields $T_c = 7.6(4)$ K. The agreement is satisfactory and thereby it demonstrates that ξ at 2 K is determined by B_{c2} near T_c. This indicates that the thermal fluctuation is relatively strong over the relevant temperature region ($T/T_c \geq 0.29$), and that the Kramer-Pesch effect must be searched for at temperatures low enough so that one may be able to neglect the temperature dependence of $B_{c2}(T)$.

V. DISCUSSION

A. Superconductivity of YB_6

Despite the early discovery of superconductivity in YB_6, there are not much literatures published so far on its superconducting property. Fortunately, a recent paper by Lortz *et al.* reports detailed measurements on specific heat, resistivity, and thermal expansion.[3] The specific heat in the sperconducting state is that typically found for a single-band, isotropic BCS superconductor, which we also confirmed on our specimen by similar measurements. Meanwhile, the electron-phonon interaction turns out to be much stronger than that in other boride superconductors such as ZrB_{12} and MgB_2. They report an enhanced coupling to phonon modes lying near 8 meV

in YB_6, which is relatively close to $\sim$ 15 meV of ZrB_{12} (Ref.24). This is to be compared with $\sim$ 60 meV in MgB_2 (Ref.25), thus it provides an explanation for the difference of T_c among those three borides. Interestingly, those low-energy frequency modes are attributed to the vibration of Y or Zr atoms loosely bound in oversized boron cages that is now called "rattling" motion. Here, the longer metal to boron bond length in YB_6 leads to a weaker force constant and larger vibrational amplitude favorable for higher T_c. The reduction of T_c under high pressure predicted from the thermal expansion measurement, which is also anticipated from the coupling to the rattling phonon, has been confirmed by the recent experiment on the pressure effect.[26]

In the previous section, we have shown that the field and temperature dependence of λ is fully consistent with the presence of isotropic order parameter in YB_6. It does not show any hint of nonlocal effect nor of low-lying quasiparticle excitation associated with the anomaly in the order parameter. This in turn suggests that the strong coupling of electrons to the rattling phonons does not necessarily lead to anomaly in the superconducting order parameter. The situation is readily understood by considering that YB_6 has a highly symmetric three-dimensional (3D) band structure, while MgB_2 is characterized by two-dimensional σ band and 3D-π band which lead to multi-gapped superconductivity (see below). However, it should be noted that the present specimen is in the dirty limit where the anisotropic feature having the length scale longer than the mean-free path ($l = 2.83$ nm, corresponding to $\hbar v_F/\pi l \sim 7$ meV assuming that $v_F \sim 10^5$ m/s) must be smeared out by scattering of electrons. Therefore, further study with much better crystal quality may be needed for the definitive conclusion.

B. η as a criterion of anomaly in the order parameter

We saw in the section IV A that the slope η of the field dependence of λ obtained by m-London model may be slightly overestimated when the model is applied beyond the presumed limit, $B/B_{c2} \leq 0.25$. This may bring about a concern on the past literatures discussing the degree of gap anisotropy by the magnitude of η. To make the situation clear, we collected results reporting the value of η obtained by using m-London model, which are shown in Fig. 9 as a plot of η versus the maximal field of measurement ($\mu_0 H_{\max}$) normalized by $\mu_0 H_{c2}$ at the measured temperature. As a comparison, those obtained by the GL model is also plotted for V_3Si (Ref.27) and YB_6 (the present result).

It is relatively well established by other experimental techniques that the group of compounds shown by the filled symbols in Fig. 9 (those with $\eta \geq 1$) have anisotropic superconducting gap or multi-gapped, except for the case of KOs_2O_6 (Refs.32,33) in which the

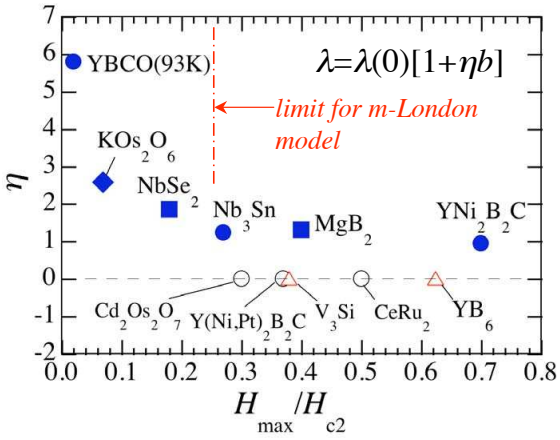

FIG. 9: Slope of field dependent λ plotted against the maximal field of measurement normalized by the upper critical field, where the m-London model was used to generate $B(r)$ (the relaxation was approximated by a Gaussian damping for $Cd_2Os_2O_7$ and MgB_2) [(Refs.8,23,27,28,29,30,31,32,33,34]. Filled symbols: superconductors with anisotropic gap (circles) or multigapped (squares). Open circles and triangles: those with isotropic gap (where the GL model was used for the latter case).

situation is not clear at this stage. While the observation that $\eta \geq 1$ for those compounds supports the use of η as a criterion for the gap anisotropy, the cases of YNi_2B_2C (Ref.28) and MgB_2 (Ref.29) might require closer examination because of large $H_{\max}/H_{c2}$. Fortunately for the case of YNi_2B_2C, data with small field step exist at lower fields ($b \leq 0.2$), and one can clearly observe that η remains to be $\simeq 1$ within the limit of m-London model ($b \simeq 0.25$). This may be partly attributed to the presence of point nodes in the superconducting order parameter[35,36] that would give rise to the nonlocal effect in YNi_2B_2C at higher fields. Since the nonlocal effect directly affects the behavior of λ, it may be less sensitive to the difference in the modeling of vortex cores between the m-London model and GL model. In particular, the situation might be that the magnitude of η at higher fields, which is predominantly determined by the nonlocal effect, coincides with that due to the Volovik effect observed at lower fields. Interestingly in $YBa_2Cu_3O_{6.95}$ (YBCO, having line nodes), it is reported that $\eta \simeq 2$ for $b \geq 0.04$ which is much smaller than $\eta \geq 5$ for $b < 0.02$ (Ref.8), where the magnitude of η at higher fields is explained by considering the nonlocal effect associated with the line nodes.[15] A similar situation would be anticipated with less magnitude of η at higher fields for the case of YNi_2B_2C with point nodes. The point node also provides a natural explanation for small η compared with that of YBCO at lower fields.

Here, it might be stressed again that there are two different sources of nonlocal effect, the one associated with the anisotropy in the superconducting order parameters and that associated with the anisotropy in the Fermi surface. In general, the latter effect manifests itself as the

transformation of FLL from hexagonal to squared with increasing external field, where transformation occurs at relatively low fields (e.g., $b < 0.06$ in YNi_2B_2C). Meanwhile, the anisotropy in the order parameter has relatively smaller energy scales and thereby it emerges at higher fields. While both yield a qualitatively similar modification to the effective London penetration depth ($\hat{L}$), their consequences are independent (even competing) with each other.[37]

It is now well established that MgB_2 is characterized by two different energy gaps corresponding to its band structure ($\Delta_\sigma \simeq 6.8$ meV for σ band and $\Delta_\pi \simeq 2.2$ meV for π band).[38] The analysis in Ref.29 was made before the revelation of the double gap, using the Gaussian approximation instead of m-London model. However, it captures anomalous behavior of $1/\lambda^2$ (proportional to the Gaussian linewidth) unexpected for the conventional superconductors with single gap.

The Gaussian model is based on a crude approximation that the Gaussian damping rate, σ, is primarily determined by the penetration depth (valid for extreme type II superconductors),

$$\sigma = \gamma_\mu \langle \sum_{\mathbf{K}} b(\mathbf{K})^2 \rangle^{1/2} \propto G(b)\lambda^{-2}, \quad (24)$$
$$G(b) \simeq (1-b)[1+3.9(1-b)^2]^{1/2},$$

where the function $G(b)$ represents the reduction of σ mainly due to the overlap of vortices (proportional to $1-b$) and additional narrowing due to the contribution of vortex cores.[6] The presence of two gaps means that there are two different upper critical fields corresponding to respective coherence length,

$$B_{c2(i)} = \frac{\Phi_0}{2\pi\xi_i}, \ (i = \sigma, \pi), \quad (25)$$

from which one may anticipate that

$$\sigma \propto [a_\sigma G(b_\sigma) + (1-a_\sigma)G(b_\pi)]\lambda^{-2}, \quad (26)$$

where $b_i = \mu_0 H/B_{c2(i)}$ (with $B_{c2(\pi)} < B_{c2(\sigma)}$), a_σ is the fractional weight of σ component, and $G(b_\pi)$ must be set to zero for $b_\pi > 1$. The second term in the above equation, which exhibits steeper field dependence than the first term, strongly reduces σ with increasing field over the field range of $0 \leq \mu_0 H < B_{c2(\pi)}$. From the viewpoint of single B_{c2}, such behavior appears as an anomalous deviation of λ from Eq.(24) and thereby easily identified as an increase of η as reported in Ref.29. As a matter of fact, recent attempt to analyze σ assuming a model similar to Eq. (26) reports $\xi_\sigma = 5.1(2)$ nm and $\xi_\pi = 23(1)$ nm.[39] Considering that the magnitude of ξ_π is as large as nearly a half of λ [=49(4) nm], the enhancement of λ is physically understood as that due to the QP's over a radial region $\xi_\sigma < r < \xi_\pi$ around vortex cores. This is presumed to be a common situation for multi-gapped superconductors including another example of $NbSe_2$.[40] We also point out that the smaller $\xi(T)$ (e.g., $\xi_\pi(T)$ in MgB_2) may exceed λ at a certain temperature, as it increases with T [see Eq. (22) and Fig 8(b)]. Then, there is a possibility that the nonlocal effect may set in to further enhance the effective λ.

Now it is clear that the magnitude of η indeed serves as a criterion for the anisotropy of superconducting order parameter, where that obtained from the analysis using the m-London model remains useful (particularly those for which the maximal field range is within the presumed limit of validity, $b < 0.25$). In this context, the previous result for KOs_2O_6 may be regarded as a strong case for the presence of anisotropic order parameter (including multi-gap) in this compound. Considering results of other experimental techniques that the order parameter is nodeless,[41] further analysis of μSR data by a model based on the double-gap scenario is now in progress.

VI. SUMMARY AND CONCLUSION

We showed that the effective London penetration depth in YB_6, obtained by analyzing μSR data using the field profile generated by the analytical GL model, is independent of external field ($\eta \simeq 0$) over a region $0 < \mu_0 H/B_{c2} < 0.65$. We made a comparative analysis using the modified London model and GL model, from which it was inferred that the GL model should be used for the precise determination of η when the field range of measurements extends over the presumed limit of validity for the m-London model ($\mu_0 H/B_{c2} > 0.25$). We also showed that the temperature dependence of $1/\lambda^2$ is perfectly in line with that predicted for isotropic BCS superconductors. This, together with the observation that $\eta \simeq 0$, supports for the conclusion drawn from bulk measurements that YB_6 belongs to the class of conventional BCS superconductors with isotropic s-wave pairing. Following this result, we re-exmined the past reports on η obtained by the analysis based on the m-London model (and those based on the Gaussian approximation), and confirmed that the conclusions drawn for respective compounds remain unchanged. Thus, the m-London model continues to be a useful ground for the μSR study of vortex state within the limit of its validity.

Acknowledgements

We would like to thank the staff of TRIUMF for their technical support during the μSR experiment. This work was partially supported by a Grant-in-Aid for Scientific Research on Priority Areas and a Grant-in-Aid for Creative Scientific Research from the Ministry of Education, Culture, Sports, Science and Technology of Japan.

[1] J. Nagamatsu, N. Nakagawa, T. Muranaka, Y. Zenitani and J. Akimitsu: Nature **410**, 63 (2001).

[2] B. T. Matthias, T. H. Geballe, K. Andres, E. Corenzwit, G. W. Hull, and J. P. Maita, Science **159**, 530 (1968).

[3] R. Lortz, Y. Wang, U. Tutsch, S. Abe, C. Meingast, P. Popovich, W. Knafo, N. Shitsevalova, Yu. B. Paderno, and A. Junod, Phys. Rev. B **73**, 024512 (2006).

[4] J. S. Tse, T. Iitaka, T. Kume, H. Shimizu, K. Parlinski, H. Fukuoka, and S. Yamanaka, Phys. Rev. B **72**, 155441 (2005).

[5] Z. Hiroi, S. Yonezawa, T. Muramatsu, J. Yamaura, and Y. Muraoka, J. Phys. Soc. Jpn. **74**, 1255 (2005).

[6] E. H. Brandt, Phys. Rev. B **37**, R2349 (1988).

[7] V. Fesenko, V. Gorbunov, A. Sidorenko, and V. Smilga, Physica C **211**, 343 (1993).

[8] J. E. Sonier, J. H. Brewer, and R. F. Kiefl, Rev. Mod. Phys. **72**, 769 (2000).

[9] E. H. Brandt, Phys. Rev. Lett. **78**, 2208 (1997).

[10] M. Laulajainen, F. D. Callaghan, C.V. Kaiser, and J. E. Sonier, Phys. Rev. B **74**, 054511 (2006). This paper seems to have some problem in their data analysis, as it reports λ and ξ obtained by comparative analysis using m-London model and two GL models (analytical and iterative) which are very close with each other, while they demonstrate poor agreement of $B(r)$ between those three models for a common set of λ and ξ.

[11] J. R. Clem, J. Low Temp. Phys. **18**, 427 (1975).

[12] A. Yaouanc, P. Dalmas de Réotier, and E. H. Brandt, Phys. Rev. B **55**, 11107 (1997).

[13] G. E. Volovik, Pis'ma Zh. Eksp. Teor. Fiz. **58**, 457 (1993) [*JETP Lett.* **58**, 469 (1993)].

[14] I. Kosztin and A. J. Leggett, Phys. Rev. Lett. **79**, 135 (1997).

[15] M. H. S. Amin, I. Affleck, and M. Franz, Phys. Rev. B **58**, 5848 (1998).

[16] R. Kadono, J. Phys.: Condens. Matt. **16**, S4421 (2004).

[17] E. H. Brandt, J. Low Temp. Phys. **24**, 709 (1977).

[18] Z. Hao, J. R. Clem, M. W. McElfresh, L. Civale, A. P. Malozemoff, and F. Holtzberg, Phys. Rev. B **43**, 2844 (1991).

[19] H. Nishimori, K. Uchiyama, S. Kaneko, A. Tokura, H. Takeya1, K. Hirata and N. Nishida, J. Phys. Soc. Jpn. **73**, 3247 (2004).

[20] S. Otani,M. M. Korsukova, T. Mitsuhashi, and N. Kieda, J. Crystal Growth **217**, 378 (2000).

[21] R. I. Miller, R. F. Kiefl, J. H. Brewer, J. Chakhalian, S. Dunsiger, G. D. Morris, J. E. Sonier, and W. A. MacFarlane, Phys. Rev. Lett. **85**, 1540 (2000).

[22] L. Kramer and W. Pesch, Z. Phys. **269**, 59 (1974).

[23] R. Kadono, W. Higemoto, A. Koda, K. Ohishi, T. Yokoo, J. Akimitsu, M. Hedo, Y. Inada, Y. Onuki, E. Yamamoto, and Y. Haga, Phys. Rev. B **63**, 224520 (2001).

[24] R. Lortz, Y. Wang, S. Abe, C. Meingast, Y. B. Paderno, V. Filippov, and A. Junod, Phys. Rev. B **72**, 024547 (2005).

[25] J. Geerk, R. Schneider, G. Linker, A. G. Zaitsev, R. Heid, K.-P. Bohnen, and H. v. Löhneysen, Phys. Rev. Lett. **94**, 227005 (2005).

[26] R. Khasanov, P. S. Häfliger, N. Shitsevalova, A. Dukhnenko, R. Brütsch, and H. Keller, Phys. Rev. Lett. **97**, 157002 (2006).

[27] J. E. Sonier, F. D. Callaghan, R. I. Miller, E. Boaknin, L. Taillefer, R. F. Kiefl, J. H. Brewer, K. F. Poon, and J. D. Brewer, Phys. Rev. Lett. **93**, 017002 (2004).

[28] K. Ohishi, K. Kakuta, J. Akimitsu, W. Higemoto, R. Kadono, J. E. Sonier, A. N. Price, R. I. Miller, R. F. Kiefl, M. Nohara, H. Suzuki and H. Takagi, Phys. Rev. B **65**, 140505(R) (2002).

[29] K. Ohishi, T. Muranaka, J. Akimitsu, A. Koda, W. Higemoto, and R. Kadono, J. Phys. Soc. Jpn. **72**, 29 (2003).

[30] K. Ohishi, K. Kakuta, J. Akimitsu, A. Koda, W. Higemoto, R. Kadono, J. E. Sonier, A. N. Price, R. I. Miller, R. F. Kiefl, M. Nohara, H. Suzuki and H. Takagi, Physica B **326**, 364 (2003).

[31] R. Kadono, W. Higemoto, A. Koda, Y. Kawasaki, M. Hanawa, and Z. Hiroi, J. Phys. Soc. Jpn. **71**, 709 (2002).

[32] A. Koda, W. Higemoto, K. Ohishi, S. R. Saha, R. Kadono, S. Yonezawa, Y. Muraoka, and Z. Hiroi, J. Phys. Soc. Jpn. **74**, 1678 (2005).

[33] A. Koda, K. H. Satoh, S. Takeshita, R. Kadono, K. Ohishi, W. Higemoto, S. R. Saha, Y. Kawasaki, T. Minami, S. Yonezawa, Z. Hiroi, and Y. Muraoka, unpublished.

[34] R. Kadono, K. H. Satoh, A. Koda, T. Nagata, H. Kawano-Furukawa, J. Suzuki, M. Matsuda, K. Ohishi, W. Higemoto, S. Kuroiwa, H. Takagiwa, and J. Akimitsu, Phys. Rev. B **74**, 024513 (2006).

[35] K. Izawa, K. Kamata, Y. Nakajima, Y. Matsuda, T.Watanabe, M. Nohara, H. Takagi, P. Thalmeier, and K. Maki, Phys. Rev. Lett. **89**, 137006 (2002).

[36] T. Watanabe, M. Nohara, T. Hanaguri, and H. Takagi, Phys. Rev. Lett. **92**, 147002 (2004).

[37] See, for example, N. Nakai, P. Miranović, M. Ichioka, and K. Machida, Phys. Rev. Lett. **89**, 237004 (2002).

[38] S. Tsuda, T. Yokoya, T. Kiss, T. Shimojima, S. Shin, T. Togashi, S. Watanabe, C. Zhang, C. T. Chen, S. Lee, H. Uchiyama, S. Tajima, N. Nakai, and K. Machida, Phys. Rev. B **72**, 064527 (2005).

[39] S. Serventi, G. Allodi, R. De Renzi, G. Guidi, L. Romanò, P. Manfrinetti, A. Palenzona, Ch. Niedermayer, A. Amato, and Ch. Baines, Phys. Rev. Lett. **93**, 217003 (2004).

[40] F. D. Callaghan, M. Laulajainen, C. V. Kaiser, and J. E. Sonier, Phys. Rev. Lett. **95**, 197001 (2005). In this paper, the authors argue that the QP's are delocalized in accordance with the shrinkage of vortex core radius. They further maintain that the situation is common to the case of V_3Si (see Fig. 4 of this paper). However, we point out that the field dependence of λ in V_3Si reported in their previous work[27] seems inconsistent with their interpretation; it remains independent of field for $\mu_0 H > 1.5$ T where the core radius undergoes shrinkage.

[41] Y. Kasahara, Y. Shimono, T. Shibauchi, Y. Matsuda, S. Yonezawa, Y. Muraoka, and Z. Hiroi, Phys. Rev. Lett. **96**, 247004 (2006).